

## **Supporting Information**

### **Bipolar Anodization Enables the Fabrication of Controlled Arrays of TiO<sub>2</sub> Nanotubes Gradient**

Gabriel Loget, Seulgi So, Robert Hahn and Patrik Schmuki\*

#### Table of Contents

##### **1-Experimental section**

- 1-1- Chemicals and Materials
- 1-2- Bipolar Anodization and Characterization
- 1-3- Photocurrent Screening

##### **2-Characterization of the annealed surfaces**

##### **3-Screening of Experimental Conditions**

##### **4-Effect of the Electrolysis Time on the Tube Diameter**

##### **5-References**

## **1-Experimental section**

### **1-1- Chemicals and Materials**

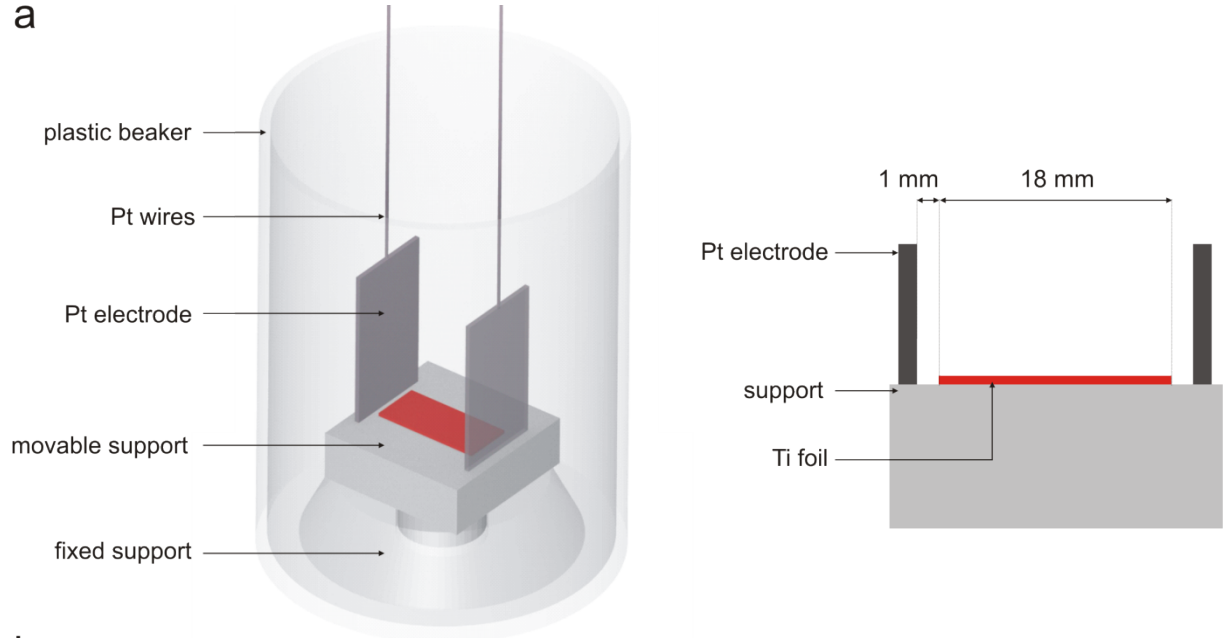
Chemicals and titanium foils (0.125 mm thick, >99.6 % purity, Advent, England) were used as received. Ethylene glycol (>99.5 %) and DL-lactic acid (90 %) were purchased from Fluka, ethanol (99.5 %) and acetone (Reag. Ph. Eur.) were purchased from Merck. Ammonium fluoride (ACS reag. >98 %) was purchased from Sigma Aldrich. The electrolyte was prepared with ultrapure water (resistivity = 17.1 mΩ.cm). For the fabrication of the arrays, Microposit S1813G2 photoresist and Microposit 351 developer were used.

For dye sensitization, annealed nanotube layers were immersed in a 300 mM solution of Ru-based dye (cis-bis(isothiocyanato)-bis(2,2-bipyridyl-4,4-dicarboxylato) ruthenium(II) bis-tetrabutylammonium) (Sigma Aldrich) in a mixture of acetonitrile and tert-butyl alcohol (1:1 v/v) for 1 day. After dye sensitization, the samples were rinsed with acetonitrile to remove non-chemisorbed dye.

### **1-2- Bipolar Anodization and Characterization**

The electrolyte used was previously developed by our lab and used for the fast growing of TiO<sub>2</sub> nanotubes.<sup>1</sup> It was composed of ammonium fluoride (0.1 M), lactic acid (1.5 M) and 5 wt% water in ethylene glycol. Titanium pieces of 2.5 x 1.6 cm (Figure 2), 2 x 0.5 cm (Figure 3 and 4) or 4 x 1.2 cm (Figure 6 and 7) were cut, degreased by sonication in acetone, ethanol and water and dried under a nitrogen stream. The description of the cell used in the experiments of Figure 3 and 4 is shown in Figure S1a and the one used for the fabrication of the gradient used in Figures 6 and 7 is shown in Figure S1b. Basically, the cells are composed of a plastic beaker in which a Teflon support has been fixed in the bottom. The Ti sample was tapped on a Teflon detachable support with Kapton tape covering 1 mm its edges in order to avoid any motion of the sample during the electrolysis as well as electrochemistry on the bottom of the foil. The support was afterwards placed in the fixed support. The electrolyte ( $\approx$ 75 mL and  $\approx$ 140 mL for the cells showed in Figures S1a and S1b, respectively) was then poured in the cell and the two feeders electrodes (platinum foils, 1.2 x 1.2 cm) were placed at a distance of 1 mm from the Ti foil edges. The experiments performed in the cell shown in Figure S1b were done under stirring. The electric field ( $E = U/d$ , with E being the electric field, U the imposed potential and d the distance between the feeder electrodes) was applied for a certain time using a LAB/SM 1300 power source (ET System). After the electrolysis, the movable support was placed in ethanol for few hours in order to remove the fluorides from the nanotubes and to detach the Kapton tape from the surface. The titanium foil was then rinsed with ethanol, water and dried under a nitrogen stream. The electrolysis cell used for the experiments performed in Figure 2 had to be adapted for video recording (performed with a Canon Ixus 210 camera). It consisted therefore of a weighting boat in which two Pt wires (feeder electrodes) have been placed. All the SEM characterizations were performed using a FE 4800 SEM (Hitachi). Photographs of the samples were taken with a Galaxy S3 mobile phone (Samsung).

a



b

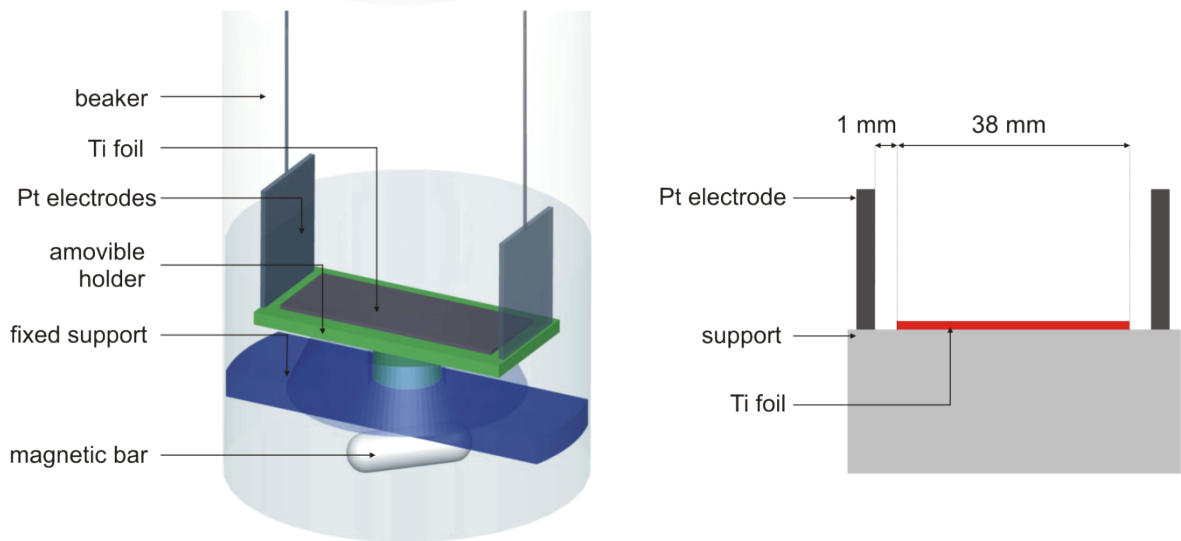


**Figure S1.** Detailed scheme (right side) and cross-section view (left side) of the bipolar electrolysis cells.

### 1-3- Photocurrent Screening

The non-TiO<sub>2</sub> parts on the surface were covered with an insulating polymer layer and the gradient was welded to an insulated Ti wire for making the electrical connection. The reference electrode was a Ag/AgCl electrode (for the experiments of Fig. 6) and a Pt electrode (for the experiments of Fig. 7) and the counter electrode a Pt foil. The counter and the gradient surface were immobilized with tape on the bottom of the cell that was filled with the electrolyte: Na<sub>2</sub>SO<sub>4</sub> (0.1 M) for the experiments shown in Fig. 6 and Iodolyte R50 (Solaronix) diluted with acetonitrile (1:4 v/v) for the experiments shown in Fig. 7. The cell was mounted on a movable stage (Karl Süss) and the laser beam:Kimmon IK Series, 200 mW (for the experiments shown in Fig. 6) or MBL 473, 20 mW (for the experiments shown in Fig. 7) was directed on the middle of the gradient using an aluminum mirror positioned on the top of the photoelectrochemical cell. A potential of +500 mV was applied to the gradient by a potentiostat (Jaissle 1030A) and the transient currents were recorded while imposing cycles of 10 s

“on” and 10 s “off” by opening and closing the laser shutter for the screening shown in Figure 6. For the screening of Figure 7, the currents were recorded after 30 s of equilibrium. The currents were measured at different positions  $x$  of the gradient. The lateral photocurrent deviation was measured at 2 positions on the sample and is shown in Figure S2.

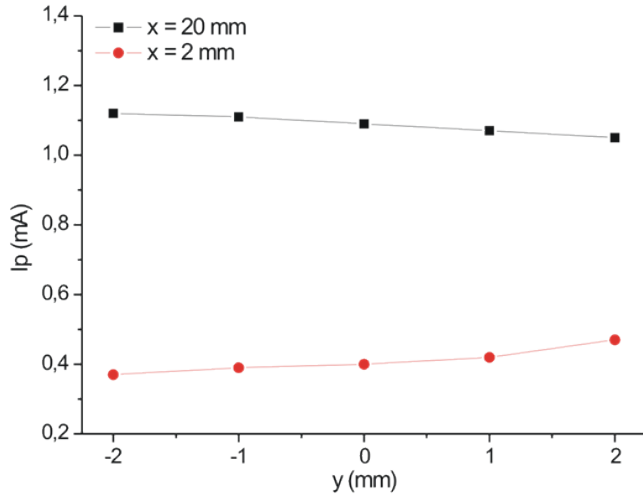


**Figure S2.** a) Curve showing the lateral photocurrent deviation along the y axis at two x positions on the sample.

## 2- Characterization of the Gradient Used for Screening

The gradient used for the screening experiments of Figure 6 was fabricated by bipolar anodization under stirring in the cell shown in Figure S1b. An electric field of  $27.5 \text{ V.cm}^{-1}$  was applied for 1 h, the delivered current and the temperature of the electrolyte were measured and are shown in Figure S4. The samples were annealed at  $450 \text{ }^{\circ}\text{C}$  in air with a heating and cooling rate of  $30 \text{ }^{\circ}\text{C min}^{-1}$  over 1 h by using a rapid thermal annealer (Jipelec JetFirst100). X-ray diffraction analysis (XRD, Xpert Philips PMD with a Panalytical X'celerator detector) using graphite monochromized  $\text{CuK}\alpha$  radiation) was used for determining the crystal structure of the samples. The spectrum is shown in Figure S5.

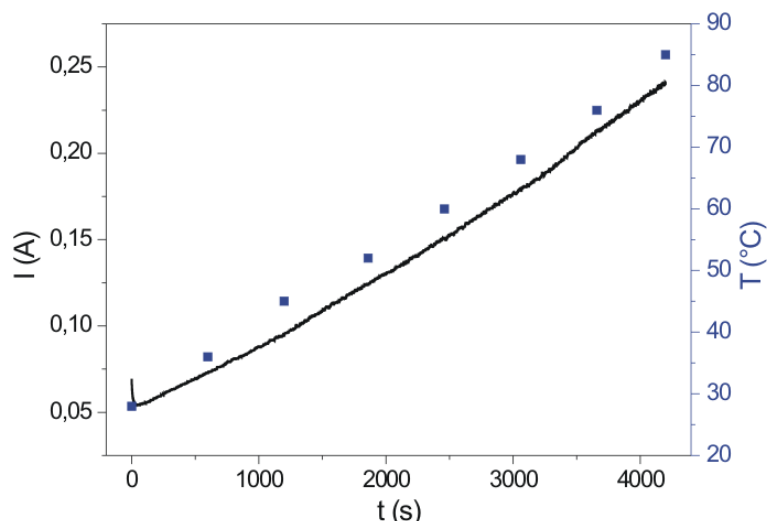


**Figure S3.** Delivered current and temperature of the electrolyte during the bipolar anodization with stirring.

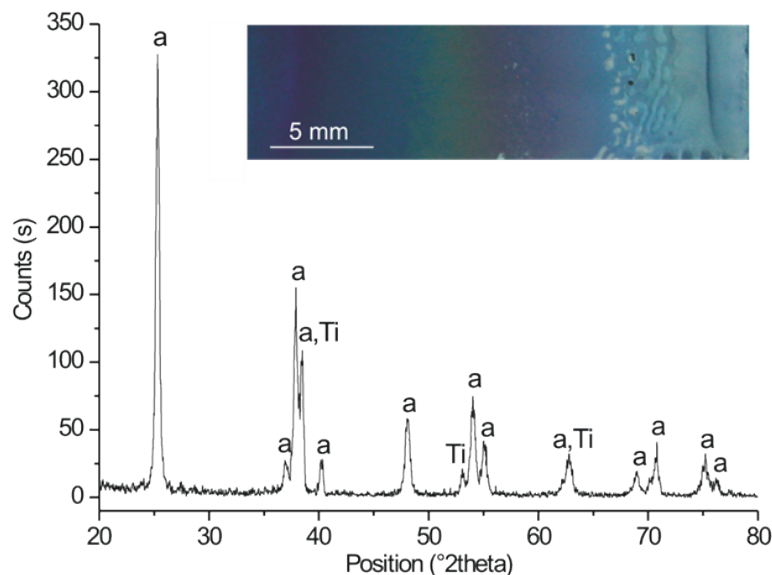


**Figure S4.** XRD spectrum of the annealed gradient. The position of the anatase peaks (a) and titanium (Ti), are indicated. Inset: Photograph of the annealed gradient.

### 3- Screening of Experimental Conditions and Measurements of the Faradaic Current

Different experimental conditions were screened and some of the obtained results are shown in Table S1. Parameters such as stirring, cooling as well as the combination of both were tested. The benefits of stirring as well as cooling is that they allowed maintaining the temperature T and the delivered current  $I_d$  at lower values, thus the electrolysis could be performed for longer time before reaching too high T values that may cause boiling of the electrolyte and liberation of hazardous side-products such as gaseous fluoridric acid. Because of the higher charge delivered during the stirred and/or cooled anodization experiments, those conditions allowed obtaining the highest length gradients. Nevertheless, they both strongly limited the growth of the tubes, with decreases of the growth rate by approximately 2 and 3 folds for stirring and cooling, respectively. Furthermore, too long anodization times ( $t \geq 30$  min) led to the formation of nanograss on the tubes, shown in Figure S5d, caused by the etching of the opening of the tubes by the fluorides.<sup>2</sup> Most of the bipolar anodizations carried out without stirring or cooling led to the classically encountered initiation layer-covered  $\text{TiO}_2$  NTs, shown in Figure S5a. In the case of bipolar double anodization, a first bipolar anodization was performed, followed by a sonication treatment for removing the tubes, which led to the creation of nanodimples on the surface. When a second bipolar anodization was performed, the tube growth was directed by the dimples, which led to the formation of an initiation layer with holes fitted with the opening of the tubes, shown in Fig S5c. It is worth mentioning that opened  $\text{TiO}_2$  NTs with a maximum value  $L_{\max} = 32 \mu\text{m}$ , shown in Figure S5b, were obtained using an electric field value of  $65 \text{ V.cm}^{-1}$  and a time of 240 s, this is explained by the increase of the etching rate of the initiation layer by the fluoride at this electric field value with respect to the experiment performed at  $55 \text{ V.cm}^{-1}$ .

**Table S1.** Study of different experimental conditions of bipolar anodization and characteristic of the obtained tubes: electric field E, time t, delivered current  $I_d$  range, temperature T, maximum length  $L_{\max}$  and the main aspect of the tube opening. Four SEM pictures of characteristic tube openings are provided in Figure S5.

| sample # | electrolysis type              | E (V.cm <sup>-1</sup> ) | t (s) | I <sub>d</sub> range (mA) | T range (°C) | L <sub>max</sub> (μm) | main aspect of the tube openings             | SEM picture of tube openings |
|----------|--------------------------------|-------------------------|-------|---------------------------|--------------|-----------------------|--|------------------------------|
| Ti32     | no stirring                    | 55                      | 400   | 70-210                    | 27-56        | 8                     | initiation layer                             | S5a                          |
| Ti39     | no stirring                    | 65                      | 240   | 90-320                    | 28-58        | 32                    | opened tubes                                 | S5b                          |
| Ti37     | no stirring-double anodization | 55                      | 240   | 60-240                    | 26-65        | 3                     | initiation layer                             | -                            |
| Ti35     | no stirring-double anodization | 65                      | 300   | 90-410                    | 27-65        | 11                    | initiation layer with better fitted openings | S5c                          |
| Ti26     | No stirring+cooling            | 55                      | 1320  | 52-300                    | 8-50         | 10                    | initiation layer                             | -                            |
| Ti19     | stirring                       | 55                      | 390   | 60-90                     | -            | 3,5                   | initiation layer                             | -                            |
| Ti22     | stirring                       | 55                      | 1800  | 90-430                    | 28-93        | 58                    | nanograss                                    | S5d                          |
| Ti25     | stirring-double anodization    | 55                      | 500   | 100-275                   | -            | >4                    | initiation layer with better fitted openings | -                            |
| Ti24     | stirring+cooling               | 55                      | 7200  | 33-93                     | 8-34         | >20                   | nanograss                                    | -                            |
| Ti27     | stirring+cooling               | 75                      | 2700  | 65-370                    | 9-60         | >24                   | nanograss                                    | -                            |

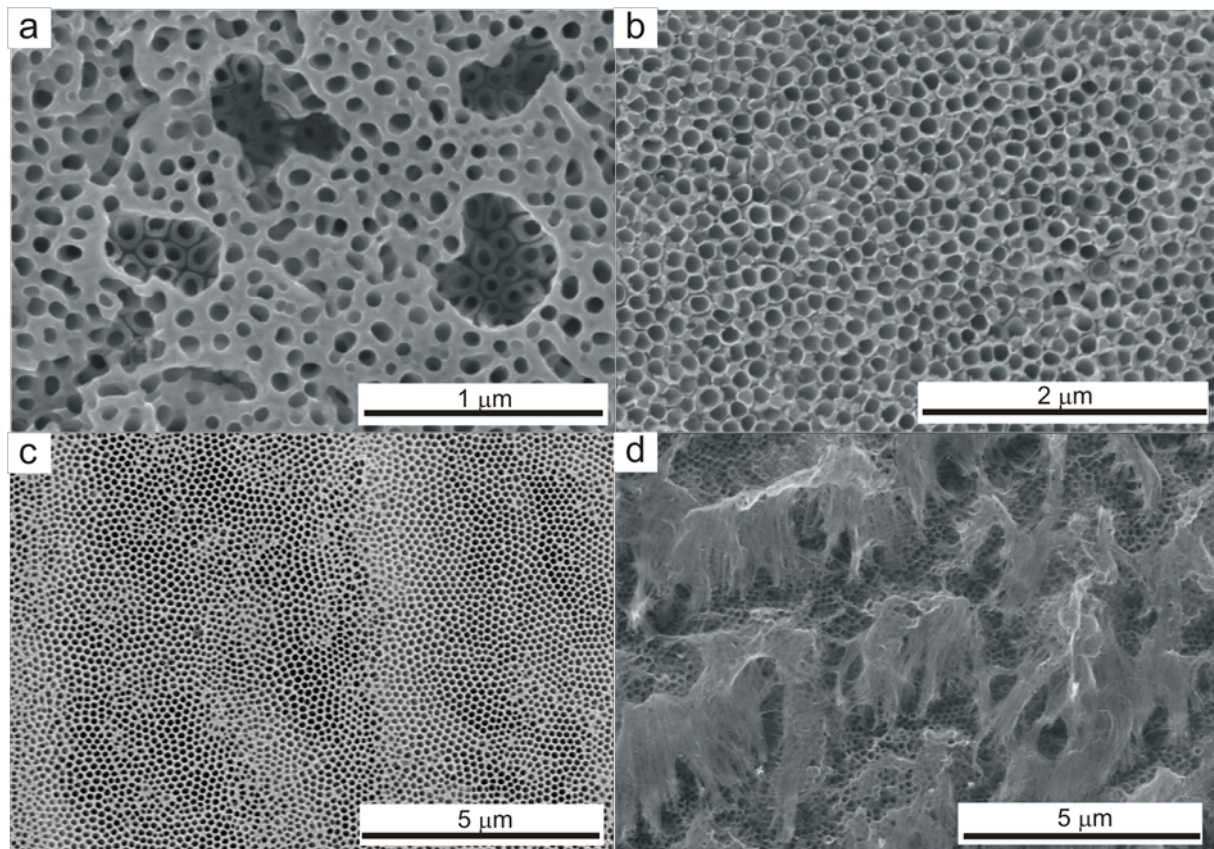


**Figure S5.** SEM top views of TiO<sub>2</sub> NT openings obtained by bipolar anodization. a) Tubes covered with an initiation layer (sample Ti32). b) Opened tubes (sample Ti39). c) Tubes covered with an initiation layer having better-fitted openings, obtained by double anodization (sample Ti35). d) Tubes covered with nanograss (sample Ti22).

#### **4-Effect of the Electrolysis Time on the Tube Diameter**

Figure S6 shows the values of the tube diameters as a function of  $x$  for samples obtained with different times of electrolysis using an electric field of  $55 \text{ V.cm}^{-1}$ .

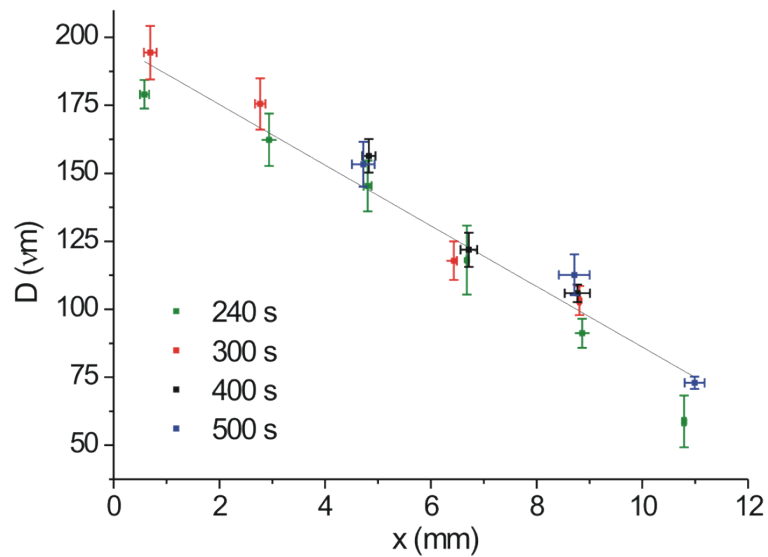


**Figure S6.** Curve showing the values of tube diameters  $D$  as a function of  $x$  for samples obtained with different times of electrolysis using an electric field of  $55 \text{ V.cm}^{-1}$ .

#### **5-References**

- 1 S. So, K. Lee, P. Schmuki, *J. Am. Chem. Soc.* **2012**, *134*, 11316-11318.
- 2 P. Roy, S. Berger, P. Schmuki, *Angew. Chem. Int. Ed.* **2011**, *50*, 2904-2939.